The DOI for this manuscript is doi: 10.1175/BAMS-D-14-00193.1

The final published version of this manuscript will replace the preliminary version at the above DOI once it is available.

If you would like to cite this EOR in a separate work, please use the following full citation:

Albrecht, R., S. Goodman, D. Buechler, R. Blakeslee, and H. Christian, 2016: Where are the lightning hotspots on Earth? Bull. Amer. Meteor. Soc. doi:10.1175/BAMS-D-14-00193.1, in press.

Where are the lightning hotspots on Earth?

Rachel I. Albrecht*
Instituto de Astronomia, Geofísica e Ciências Atmosféricas, Universidade de São Paulo, Sao Paulo, Brazil
CICS University of Maryland, College Park, MD

Steven J. Goodman
NOAA National Environmental Satellite Data and Information Service, Greenbelt, MD

Dennis E. Buechler
University of Alabama in Huntsville, Huntsville, AL

Richard J. Blakeslee
NASA Marshall Space Flight Center, Huntsville, AL

Hugh J. Christian
University of Alabama in Huntsville, Huntsville, AL

May 2015 (Revised September, 2015; Revised January, 2016)

To be submitted to *Bulletin of American Meteorological Society*

* Corresponding author:

Prof. Dr. Rachel Ifanger Albrecht, Universidade de Sao Paulo, Rua do Matao, 1226, Sao Paulo – SP 05509-090 Brazil. E-mail: rachel.albrecht@iag.usp.br, phone: +55 (11) 3091 4738.

Capsule

The earth's total lightning hotspots are revealed with very high resolution lightning climatology derived from 16 years of space-based Lightning Imaging Sensor observations. The peak hotspot occurs in Venezuela over Lake Maracaibo.

Abstract

Previous total lightning climatology studies using TRMM Lightning Imaging Sensor (LIS) observations were reported at coarse resolution (0.5°) and employed significant spatial and temporal smoothing to account for sampling limitations of TRMM's tropical to sub-tropical low-earth orbit coverage. The analysis reported here uses a 16 year reprocessed data set to create a very high resolution (0.1°) climatology with no further spatial averaging. This analysis reveals that the Earth's principal lightning hotspot occurs over Lake Maracaibo in Venezuela, while the highest flash rate density hotspot previously found at the lower 0.5° resolution sampling was found in the Congo Basin in Africa. Lake Maracaibo's pattern of convergent windflow (mountain-valley, lake and sea breezes) occurs over the warm lake waters nearly year-round and contributes to nocturnal thunderstorm development 297 days per year in average. These thunderstorms are very localized and their persistent development anchored in one location accounts for the high flash rate density. Several other inland lakes with similar conditions, i.e., deep nocturnal convection driven by locally forced convergent flow over a warm lake surface, are also revealed.

Africa is the continent with the most lightning hotspots, followed by Asia, South America, North America, and Australia. A climatological map of the local hour of maximum flash rate density reveals that most oceanic total lightning maxima are related to nocturnal thunderstorms, while continental lightning tends to occur during the afternoon. Most of the principal continental maxima are located near major mountain ranges, revealing the importance of local topography in thunderstorm development.

Text (up to 4500 words)

The Earth's lightning flash frequency has been an object of interest and study for decades. The first estimate of the global lightning flash rate was 100 flashes per second (fl s^{-1}) based on an average number of lightning flashes per storm and thunderstorm counts recorded by several surface weather stations (Brooks 1925). In subsequent years, human observers, individual flash counters, regional-continental ground-based lightning location networks, and finally earth-orbiting instruments were used by several authors to estimate global flash rates (WMO 1953; Kotaki 1984; Orville and Henderson 1986; Goodman and Christian 1993; Williams and Heckman 1993; Heckman et al. 1998; Mackerras et al. 1998; Boccippio et al. 2000; Williams et al. 2000; Christian et al. 2003; Albrecht et al. 2014). Ground-based radio frequency measurement systems provide reliable lightning location, but offer limited spatial coverage, especially over the oceans and the tropics. These systems detect predominantly cloud-to-ground lightning relying on land-based receivers that are at great distances from where lightning is striking. It was not until the satellite era that consistent monitoring of total lightning (i.e., cloud-to-ground and intracloud) was possible at the planetary scale. The first lightning observations from space are dated from the early 1960s using both optical and radio frequency sensors. More than a dozen spacecraft orbiting the Earth have flown instruments that recorded signals from thunderstorm lightning over the past 45 years. These instruments generally had low spatial resolution, low detection efficiency and were unable to provide precise measurements of lightning characteristics (Christian et al. 1992; Goodman and Christian 1993).

In 1995, NASA launched the Optical Transient Detector (OTD) – a prototype of the Lightning Imaging Sensor (LIS) instrument – as a hosted payload onboard the Microlab-1 (later renamed as OrbView-1) small communications satellite. The OTD was the first instrument specifically designed to detect lightning from space during both day and night with storm scale resolution (Christian et al. 2003). In a low Earth orbit inclination of 70^o and at 740 km of altitude, OTD observed individual storms in a region 1300 km x 1300 km for about 3 minutes during each satellite overpass, between 1995 and 2000. The result is an annual global flash rate estimate of 44 fl s^{-1} with a maximum of 55 fl s^{-1} in the boreal summer and a minimum of 35 fl s^{-1} in the austral summer (Christian et al. 2003). The Lightning Imaging Sensor (LIS) onboard the NASA Tropical Rainfall Measuring Mission (TRMM) was launched in November 1997 into a precessing orbit inclination of 35° at an altitude of 350 km[1]. From this orbit an individual storm within the LIS field-of-view of 600 km x 600 km was observable for about 90 sec. The LIS instrument has shown no discernible degradation during its time in orbit (Buechler et al. 2014). The LIS was powered off and the TRMM mission ended data collection on April 8, 2015, thus extending what was originally a three year mission for a total of 17+ years.

The overall measurement objective of LIS was to supply further insights into the nature of tropical oceanic and continental convective clouds, providing the basis for the development of a comprehensive global thunderstorm and lightning climatology. With this focus, total lightning observed from OTD and LIS have been used to analyze global and regional thunderstorm electrical activity (e.g., Boccippio et al. 2000; Goodman et al. 2000; Williams et al. 2000; Christian et al. 2003; Cecil et al. 2005; Petersen et al. 2005; Zipser et al. 2006; Liu et al. 2011; Cecil et al. 2014). Based on five years of OTD and three years of LIS measurements, Christian et al. (2003) and Boccippio et al. (2000) presented the first detailed lightning climatology maps, which described the frequency and distribution of lightning over the globe and the tropics, respectively. These authors were pioneers in constructing comprehensive total lightning

[1] TRMM was boosted to 402 km of altitude in August 2001 to extend the mission lifetime.

climatologies using a 0.5^{o} resolution for annualized composite and 2.5^{o} resolution for decomposition of the annual cycle. To overcome limited sampling in places with low flash rates such as oceans, arid regions and higher latitudes sampled only by OTD, these climatology maps have substantial spatial and temporal smoothing as well as low pass digital filtering. Christian et al. (2003) and Boccippio et al. (2000) found that the greatest flash rates occur indeed in the tropical region along coastal areas, mountainous regions, regions with frequent extra-tropical synoptic scale cyclones, and large-scale convergence zones (South Atlantic, South Pacific and Intertropical Convergence Zones). Based on the smoothed 0.5^{o} resolution total lightning map from OTD, Christian et al. (2003) declared the equatorial Congo Basin as the lightning hotspot of the planet, more specifically at Kamembe, Rwanda, in the top place, and several locations in the Democratic Republic of Congo as well as Nigeria, Gabon, Madagascar and Cameroon. In South America, the principal lightning hotspots were located in northern Argentina extending towards Paraguay and Brazil, along one of the regions of most intense thunderstorms on Earth (Cecil et al. 2005; Zipser et al. 2006) and a few isolated locations in Colombia, Brazil and Peru. In Asia, Kuala Lumpur, Malaysia, stood out as the place with most lightning occurrence, in Australia Fitzroy Crossing and in North America, Tampa, FL. Boccippio et al. (2000) also revealed the Congo Basin as the region with the highest flash rate per thunderstorm cell.

A merged global lightning 0.5^{o} resolution data set comprised of individual LIS and OTD orbits has been updated each year and is freely available online[2] (Cecil et al. 2014). This LIS-OTD climatology is the most accurate depiction of total lightning across the planet to date, named the HRAC - *High resolution annual climatology* database. Following the methodology of Christian et al. (2003) and Boccippio et al. (2000), the HRAC climatology also has spatial (2.5^{o}

[2] http://lightning.nsstc.nasa.gov/data/data_lis-otd-climatology.html

moving average) and temporal (55 days moving average) smoothing and low pass digital filtering. Cecil et al. (2014) reconfirm the earlier lightning flash rate climatology, with a mean global flash rate of 46 fl s^{-1} (varying from around 35 fl s^{-1} in austral summer to 60 fl s−1 in boreal summer) with a peak annual flash rate of 160 fl km^{-2} yr^{-1} over the eastern Congo basin.

In this paper, we depict a very high resolution total lightning climatology gridded at 0.1° using 16 years (1998-2013) of observations from LIS. We used individual LIS orbit data files available from the NASA EOSDIS Global Hydrology Resource Center (GHRC) (http://ghrc.nsstc.nasa.gov/). TRMM started its descending path to decommissioning in 2014 with several instrument outages during the period which we expect could introduce uncertainties on the climatology, ranking and annual and diurnal cycles presented in this study. Therefore, 2014 and 2015 data were not included in this study. The focus of this paper is to identify the Earth's lightning hotspots and other regional features revealed by a detailed very high resolution satellite-derived climatology. The targets of our analysis are the places where most lightning occurs, i.e., the lightning hotspots on Earth. Therefore, no temporal or spatial smoothing is applied to the lightning climatology to best reveal the specific location of lightning hotspots tied to orographic features. The methodology to derive the climatology in this study is similar to that used in the previous satellite depictions (Christian et al. 2003; Cecil et al. 2014), but at higher resolution and no spatial smoothing to the full climatology dataset (besides the intrinsic smoothing of gridding data). This climatology is called the LIS *Very High Resolution Climatology* and is comprised of five datasets: VHRFC (Very High Resolution Full Climatology), VHRDC (Very High Resolution Diurnal Climatology), VHRMC (Very High Resolution Monthly Climatology), VHRMC (Very High Resolution Seasonal Climatology), and VHRAC (Very High Resolution Annual Cycle). Each dataset has the FRD and VT gridded fields, all compiled with LIS data from 1998 to 2013. A full description of these fields and the details on the computation of this 0.1° resolution climatology, as well as its uncertainties, can be found in the *Online Supplement Material* (OSM) accompanying this article. The datasets and figure maps from this manuscript are publicly available and hosted by the Global Hydrology Resource Center (GHRC) at https://ghrc.nsstc.nasa.gov/pub/lis/climatology/LIS/ **(DATA D.O.I. TO BE INCLUDED HERE).** It is imperative that potential users of this dataset read the OSM to better understand the insights of the total climatology computations.

TRMM LIS VERY HIGH RESOLUTION FULL CLIMATOLOGY (VHRFC)

The TRMM LIS total lightning flash rate density (FRD – fl km^{-2} yr^{-1}) climatology map from 16 years (1998-2013) of observations, and in very high horizontal (0.1°) resolution is shown in Figure 1. Figure 1 also shows the local time of maximum FRD and the month of maximum FRD. As expected, the large scale features of tropical thunderstorm activity found by Boccippio et al. (2000), Christian et al. (2003) and Cecil et al. (2014) are still captured here at 0.1° resolution. The difference between land and ocean can be clearly observed by intense convection occurring more frequently over the continents than the oceans, mainly due to the lower heat capacity of land, where the ground can warm the air more effectively increasing convective updrafts (Williams and Stanfill 2002; Williams 2004; Futyan and Del Genio 2007). In general, the local standard time (LST) and month of maximum lightning activity (Figures 1b and 1c, respectively) over land occur during the afternoon (12 to18 LST) and the hemisphere summer trimester (December-January-February in the Southern Hemisphere and June-June-August in Northern Hemisphere). However, some coastal-oceanic regions present moderate FRD (up to 30 fl km^{-2} yr^{-1}) associated with frequent synoptic scale extra-tropical cyclones and cold fronts (such as south-southeast coasts of Brazil, South Africa, Australia) that occur throughout the year and at all times of the day (i.e., there is a negligible or non-existent annual and diurnal cycle). Moderate lightning activity is also observed at the warm Gulf Stream at the southeast U.S. coast, with a maximum during boreal summer. This particular coastal region has twice the number of lightning flashes, days and hours during El Nino years than non El Nino years (Goodman et al. 2000).

Monsoonal regions such as the Amazon and Indian subcontinent have the most lightning activity during spring, considered the pre-monsoon phase (Williams 2002; Kandalgaonkar 2003; Kodama et al. 2005; Petersen et al. 2006; Lal and Pawar 2009; Albrecht et al. 2011b). The Indian subcontinent as a whole has a lightning maximum during the pre-monsoon season and a secondary peak in late August to October (Kandalgaonkar 2005; Lal and Pawar 2009). This second peak is related to thunderstorms during the post-monsoon season in the central region, also shown in Figure 1c.

Regions where thunderstorm activity is dominated by land-sea breeze interactions show high lightning activity (30 to 50 fl km^{-2} yr^{-1}) over land near the coast (Figure 1a), where the maximum thunderstorm activity occurs during afternoon (13-17 LST) (Figure 1b) and during the summer (Figure 1c). At night, offshore wind flow develops thunderstorms over the oceans near coastal regions with low (6 to 10 fl km^{-2} yr^{-1}) to moderate (10 to 30 fl km^{-2} yr^{-1}) lightning activity. Several pronounced examples of this are found in the coastal regions of the continents and islands in Central America and the Maritime Continent. One noticeable example is the Strait of Malacca, a narrow stretch of water between the peninsular Malaysia and the Sumatra Island (Indonesia). During the day, onshore breezes foment convergence and thunderstorm development over the island, while during the night, the offshore breeze blows from both landmasses towards the Strait of Malacca, converging over warm sea water and driving nocturnal thunderstorms (more details in the next section). The presence of enhanced nocturnal ice scattering from clouds at the Strait of Malacca has been reported by Nesbitt and Zipser (2003), and Virts et al. (2013) reports high cloud-to-ground lightning activity during the night in this same region. Nocturnal lightning is also observed at regions with complex terrain, such as in the Andes (especially in Colombia) and the Himalayas (Virts et al. 2013). Moreover, nocturnal and early morning moderate to high lightning activity is found in the central-southern US Great Plains, northern Argentina, Southeast Asia and West Africa. These regions produce large mesoscale convective systems (MCS) predominantly during spring time (Figure 1c) with maximum convective activity during the night (Laing and Fritsch 1997; Kodama et al. 2005; Rasmussen and Houze 2011; Rasmussen et al. 2014).

Places with very high FRD (higher than 50 fl km^{-2} yr^{-1}) are extensively located over the Congo basin, the coastal zones of Cuba, Saudi Arabia and Yemen, and near several mountain regions, such as the Andes, Sierra Mountains, western highlands of the Cameroon line, Mitumba Mountains, Himalayas, and mountain ranges in Indonesia and Papua New Guinea. It is over these complex terrain regions that most of the Earth's lightning hotspots are located. These hotspots are ranked and identified in the following section.

LIGHTNING FLASH RATE DENSITY RANKING AND CONTINENTAL LANDMASSES HOTSPOTS

The individual 0.1° total lightning flash rate density grid boxes from Figure 1 were ranked from highest to lowest values and associated to a populated place name with more than 1,000 inhabitants from the geographical database GeoNames (http://www.geonames.org/). In order to minimize an excessive number of identical place names within clusters of very high flash rate density (>50 fl km^{-2} yr^{-1}), such as Africa and northern region of South America, a criterion of a minimum distance of 100 km between maxima is applied. Therefore the identified lightning hotspots should be interpreted as a cluster of hotspots around a reference location. Also, it may exclude popular and well-known locations as it chooses the closest populated place and not the place with the most inhabitants. More details on the ranking methodology and the complete list of the first 500 hotspots are shown in the online supplement material. In Table 1 we show the top ten lightning hotspots for each continental landmass covered by LIS (North America, South America, Africa, Asia and Oceania). Figure 2 shows the geographical distribution of the top ten lightning hotspots of each major tropical continental landmass as well as a zoomed plot of the total lightning climatology (refer to Figure 1) at each first continental landmass hotspot. Note that LIS measurements are limited to approximately ± 38° such that continents are not observed in their entirety. The rankings are based on the portions of the continents observed by LIS.

Not surprisingly, Africa is represented by 283 of the top 500 places with the highest lightning frequency, followed by Asia with 87, South America with 67, North America with 53 and Oceania with 10 (Table 1 of OSM). However, one surprising discovery is that the Earth's top-ranked total lightning hotspot is not in Africa as reported previously, but instead directly over Lake Maracaibo in Venezuela [9.75°, -71.65°] where 233 fl km^{-2} yr^{-1} occur, leaving the previously identified Congo Basin hotspot in Africa (Christian et al. 2003; Goodman et al. 2007;

Cecil et al. 2014) in second place with 205 fl km^{-2} yr^{-1}. The closest populated place to this hotspot over Lake Maracaibo is Lagunillas in the state of Zulia on the east side of the lake, about 60 km away. Figure 2 shows that the Earth's top-ranked maximum over Lake Maracaibo is very localized, covering an area of approximately 5,500 km^2 with FRD greater than 50 fl km^{-2} yr^{-1}. This corresponds to only 45 pixels in 0.1° resolution and less than 2 pixels in 0.50° resolution and explains why it was not similarly identified in the previous lower resolution (0.5°) LIS climatologies of Christian et al. (2003) and Cecil et al. (2014) (more details on the OSM). The diurnal and annual cycles of lightning activity over Lake Maracaibo and other landmass hotspots are shown in Figure 3. Lightning activity over Lake Maracaibo presents two peaks during the year, where most of lightning occurs from August to November (>65 fl day^{-1}), drastically decreasing in December with almost no lightning in January and February. The second peak is an approximately flat flash rate (47 fl day^{-1}) in May and June and is related to the migration of the Intertropical Convergence Zone (ITCZ) (Pulwarty et al. 1998). The strong diurnal cycle of lightning frequency reveals almost no lightning during the day and a nocturnal maximum (>2.5 fl h^{-1}) from 00 to 05 LST abruptly peaking (5.4 fl h^{-1}) at 03 LST (Figure 3a).

South America

Seven of South America's top ten hotspots (including the Earth's top hotspot at Lake Maracaibo) are located near or at the valleys or foothills of the northern Andes Mountains in Colombia, Venezuela and Bolivia (Figure 2). All these hotspots, except the one in Bolivia, have similar annual and diurnal cycles of lightning activity (Figures 1c and 3a), with most lightning activity (>15 fl day^{-1}) from austral fall (MAM) through austral spring (SON) with a peak in

August or September (37 to 88 fl day^{-1}), and most lightning occurring during the night (>2 fl h^{-1}). Nocturnal maxima of deep convection were also observed by other authors over the valleys along the most northern portion of the Andes Mountains, including Lake Maracaibo (Garreaud and Wallace 1997; Negri et al. 2000; Mapes et al. 2003a; Poveda et al. 2005; Bürgesser et al. 2012; Virts et al. 2013). These authors attributed the nocturnal convection to local thermally driven circulations (land-sea breezes and mountain-valley breezes) that provide low-level convergence inside the valleys and offshore (Gulf of Panama), as well as convergence of gravity waves from diurnally varying heat sources (differential heating between land, lake, mountain and valleys) (Mapes et al. 2003a). Lightning activity in the Bolivian hotspot (Chimoré) is from austral spring to summer (>5 fl day^{-1}, peaking in November – 30 fl day^{-1} – Figure 3b) without a well-defined diurnal cycle (0.5-1.0 fl h^{-1} from 1300 to 0400 LST – Figure 3a). This hotspot is also at the Andes' foothills, at the end of the northwest-southeast orientated range, inside Carrasco National Park. In this configuration, the mountains are a natural barrier to the moist easterly winds from the Amazon basin, forcing it uphill and favoring thunderstorm development during spring and summer. Inferred peaks of hailstorm frequency, based on passive microwave observations from satellite, were also found by Cecil and Blankenship (2012) at this same spot during spring and summer. Four hotspots (sixth, seventh, ninth, and tenth) are located near the Colombia and Venezuela coasts, presenting the same annual cycle as most of the top ten South America hotspots. However, those hotspots further to the west (seventh and ninth) have afternoon peaks (> 2 fl h^{-1}) at 1700 LST due to a well-defined diurnal cycle and sea breeze near elevated terrain (Figure 2 – South America zoom at Lake Maracaibo).

Africa

Earth's second greatest lightning hotspot is at Kahuzi-Biéga National Park [-1.85°, 27.75°], 136.2 km northwest of Kabare in the Democratic Republic of Congo near the border of Rwanda, on the west side of the Mitumba Mountains (Figure 2). The Mitumba Mountains at the eastern edge of the Congo Basin mark the beginning of the Western Rift Valley in East Africa, along a north-south orientation at ~29°E and with peaks ranging from 2000 to 5200 m. Total lightning flash rate densities greater than 50 fl km^{-2} yr^{-1} are observed along a continuous large area (~320,000 km^2) on the western foothills of these mountains from 4°S to 5°N, having six out of the ten African hotspots. The FRD decreases westward of 25°E to a narrow region of 40-50 fl km^{-2} yr^{-1} and increases again to over 50 fl km^{-2} yr^{-1} (Figure 1) having two other African hotspots. All the hotspots over the Mitumba Mountains exhibit higher mean diurnal cycle flash rates (Figure 3b) during the afternoon (peak of 5 fl h^{-1} from 15 to 17 LST) than in the Central Congo (~3 fl h^{-1} at 15 LST), with some activity during the night (~1 fl h^{-1}) associated with the maximum extent of MCSs (Laing and Fritsch 1993; Jackson et al. 2009).

Thunderstorms occur year round in Central and Western Africa, but these regions are electrically more active from September through May, with flash rates over 15 fl day^{-1} occurring on most days, with less lightning activity observed in July (Figure 3b). The spatial and temporal distributions of African rainfall, and therefore also lightning activity, are tied to a combination of large and local scale factors, such as the seasonal migration of the ITCZ, the position of the African Easterly Jets (which migrate seasonally with the ITCZ and are evident from August to November), long nocturnal life cycle of MCSs, afternoon boundary layer destabilization, local effects of sea breezes and topography, as well as the sea surface temperatures (Nicholson 1996; Yin and Nicholson 2000; Nicholson and Grist 2003; Balas and Nicholson 2007; Jackson et al. 2009; Nicholson 2009). Particularly, from August to November, the African Easterly Jet of the

Northern Hemisphere (AEJ-N) and the African Easterly Jet of the Southern Hemisphere (AEJ-S) are well developed, and located, respectively, above and below the edges of the Mitumba Mountain range. In addition, there is a strong low-level moisture convergence on its lee side, coming from the Atlantic and Central Congo rainforest (Jackson et al. 2009). This mesoscale configuration results in a convergence region with strong vertical motions on the right entrance of the AEJ-S, which along with the deep low-level moisture source, promotes an explosive convection scenario for thunderstorm and lightning development over the whole of the Congo Basin (Nicholson 1996; Jackson et al. 2009). This is reflected in the lightning maximum ranking (Table 1), where 8 of the 10 most active lightning places in Africa occur within the Democratic Republic of Congo, all having FRD greater than 110 fl km^{-2} yr^{-1}. The two African hotspots at the Cameroon border (Nguti, CM and Baissa, NG) have their diurnal cycle influenced by local afternoon convection driven by sea breeze and moisture flux convergence from the Gulf of Guinea (Nicholson 2009).

Asia

High to very high FRD (>30 fl km^{-2} yr^{-1}) can be found at the high elevation envelope along the length of the Himalayas in Asia. Asia's top-ranked lightning hotspot, Daggar, Pakistan [34.45º, 72.35 º], is located in the westernmost portion of the Himalayas foothills at the Indus' Plain, more specifically at the Hindu Kush Mountains on the northernmost region of Pakistan (Figure 2). Three other Asian hotspots (the second, third and fifth highest) are also located in this region, whereas the sixth Asian hotspot is at the most eastern portion of Himalayas, at Kashi Hills (on the border between India and Bangladesh). The western Himalayas were also identified as a region with the most intense thunderstorms on Earth by Cecil et al. (2005), Zipser et al. (2006), and Houze et al. (2007). Houze et al. (2007) found that the deepest intense convective storms occur upwind or at the foothills of the mountains, where the moist southwesterly monsoon flow from the Arabian Sea meets the descending dry air from the Afghan or Tibetan Plateaus, suggesting a similarity to dryline convection. All these hotspots have more lightning activity (> 15 fl day^{-1}) during the monsoon months (May-October, peaking in September – Figure 3) and less from November until March, with the most lightning activity extending from late afternoon (16 LST) to early morning (06 LST), with the exception of the second and third ranked hot spots. The nocturnal lightning is controlled by a few MCSs and local convection induced by the interaction between the large scale synoptic flow and the complex terrain (Barros and Lang 2003; Barros et al. 2004; Zipser et al. 2006; Houze et al. 2007). Barros et al. (2004) found that two types of orographic terrain control cloudiness in the Himalayan range: the first type is associated with the major river valleys (~300 km wide) and the overall mountain range that connects India and the Tibetan Plateau, while the second type is associated with the succession of ridges and small valleys (5-150 km wide). In fact, Figure 1a shows a long nearly contiguous line and a broken line of FRD greater than 30 km^{-2} yr^{-1} within the Himalayan river valleys and the narrow valleys, respectively, in North India and Nepal, with an indistinct local hour of maximum lightning activity (Figure 1b) at night and early morning. At high elevations and the Tibetan Plateau the local hour of maximum is during the day.

The remaining Asia hotspots, except for one in Yemen, lie over the coasts of Malaysia and Sumatra Island (Indonesia) and are caused by a sea breeze resulting in the afternoon (peak at 15 LST – Figure 3a) in FRD. Figure 4 shows daytime and nighttime FRD over Malaysia and Sumatra Island. High FRD greater than 50 fl km^{-2} yr^{-1} is found inland, alongside the coast and high elevated terrain. During the night, convergent offshore breezes from the peninsular Malaysia and the Sumatra Island over the Strait of Malacca leads to increased FRD over the ocean after midnight (Figure 1b). The annual cycle shows two peaks during the year associated with the ITCZ migration from the Northern to the Southern Hemispheres (Figure 3b). The hotspot at Yemen (Al Ḩadīyah, [14.55º, 43.45 º]) also presents a maximum of activity in the afternoon due to sea breeze, but its annual cycle shows lesser lightning activity (<30 fl day^{-1}) peaking in August.

North America

In North America, the first and second hotspots with FRD > 100 fl km^{-2} yr^{-1} (respectively, Patalul and Catarina, in Guatemala) as well as the ninth hotspot (Rosamorada, Mexico) are also at the foothills of a mountain range, the Sierra Madre, in a very narrow low level strip of land between the Pacific Ocean and the mountains. These hotspots show an afternoon lightning peak with most of the lightning activity occurring during boreal spring and summer. All remaining North American hotspots are over the Central America islands (Cuba, Honduras, Haiti and Jamaica) which also exhibit afternoon lightning activity occurring mostly during spring and summer.

The top United States hotspot with a FRD of 79 fl km^{-2} yr^{-1} lies over the Everglades near Orangetree, Florida, about 37 km from Fort Meyers. The top US hotspot is ranked only 14^{th} in North America (122^{th} globally). This same location coincides with that found in the first thunderstorm day climatology constructed by Court and Griffiths (1983). These authors compiled the number of thunderstorm days recorded by surface weather stations around the globe from 1951 to 1975, and found that Fort Meyers, Florida, is the place with the most thunderstorm days per year (96) in the United States, with a peak in July.

Oceania

Oceania hotspots all are found at the northern coast of Australia, except the 5th most active locale which is found in Papua New Guinea. Most of the FRD across Australia and Papua New Guinea is less than 10 fl km^{-2} yr^{-1}, and is attributable to local convection in the afternoon, mostly during austral summer monsoon with two peaks (December and mid-January to March – Figure 3b) (Jayaratne and Kuleshov 2006; Kuleshov et al. 2006), in contrast to the other two monsoonal regimes of the Amazon and India which exhibits lightning peaks during pre-monsoon. The diurnal cycle of the hotspot at Ambunti, Papua New Guinea, also exhibit lightning maximum during the afternoon (Figure 3a), but its annual cycle shows much lower FRD than Australia, peaking two months earlier (October) than Australia hotspots. It is worthwhile to note that North America's and Oceania's top hotspots have a FRD that is barely on the order of the Africa's tenth ranked hotspot (~100 fl km^{-2} yr^{-1}). This reflects the greater occurrence of convection and lightning activity in tropical belts of Africa, South America and Asia.

EARTH'S TOP LIGHTNING HOTSPOT

Nocturnal thunderstorms over Lake Maracaibo are so frequent that their lightning activity was used as a lighthouse by Caribbean navigators in colonial times (Codazzi 1841), and they are also mentioned in the La Dragontea (1598) poem, from the Spanish poet Felix Lope De Vega, as what prevented an English pirate to attack Maracaibo. These thunderstorms are locally known as the "Lighthouse of Catatumbo", "The Never-Ending Storm of Catatumbo", or simply "Catatumbo lightning". Catatumbo is a river that ends southwest of Maracaibo Lake, and nowadays tourists can take nighttime boat tours to observe these beautiful storms.

Lake Maracaibo has a unique set of features that contributes to the development of deep convection at the same place 297 days per year on average (Figure 3b) with a maximum at night (Figure 3a). This lake is the largest in South America, with an area of 13,210 km^2, and is located between the most northern ridges of the Andes Mountains (Figure 5). At its northern portion, Andean Mountains are branched out defining several large valleys over Colombia, and form a valley in which lies Lake Maracaibo. The lake is connected to the Gulf of Venezuela at its northern end, near Maracaibo city, and the very warm water temperatures over the lake and at the gulf throughout the year (28 to 31ºC), with maximum in September (Muñoz et al. 2008), serving as a great source of heat and moisture for convection.

All these geographical features combined with convergent wind flow (mountain-valley, lake and land-sea breezes) over this warm, humid lake within the ITCZ make an ideal spot for thunderstorm development. During the day, radiative heating by the sun causes the land surrounding the lake to become hotter than the lake, inducing a lake breeze circulation with subsidence over Lake Maracaibo. In addition, the sides of the mountains warm up more rapidly than the valley thereby inducing a valley breeze accompanied by subsidence over the lake inhibiting convection. This can be seen in the diurnal distribution of FRD over this region in Figure 6a. Lightning activity is only observed over a small area of the lake during the late afternoon. Most of the daytime lightning occurs near the coast and is driven by a sea breeze circulation that is forced uphill to higher elevations. On the other hand, during the night, radiative cooling causes the land to become cooler than the lake with the surrounding mountainsides cooling more rapidly than the valley, yielding a low-level wind convergence over the hot and humid environment of the lake.

Figure 5 shows wind roses (frequency of wind speed by wind direction) of surface weather station data during daytime (07-18 LST) and nighttime (19-06 LST) at three locations around Lake Maracaibo (Zulia, Mene Grande and Maracaibo) for the period 1998 to 2014. This dataset is freely available online through NOAA National Climate Data Center's Integrated Surface Database (ISD) (https://www.ncdc.noaa.gov/isd) .ISD consists of surface observations from over 35,000 stations worldwide compiled from numerous sources into a single common data format (Lott et al. 2008).). It can be seen that, in general, the wind indeed blows towards the lake during the night and away from the lake during the day. This results in a nighttime convergent land-lake breeze and a daytime divergent lake-land breeze over the lake. This is a perfect combination for nocturnal thunderstorm development and very high flash rate occurrence, where FRD above 50 fl km^{-2} yr^{-1} covers most of the lake area, the southwestern portion of the valley and also several valleys in Colombia during nighttime (Figure 6a).

The two flash rate peaks from August to October and May to July coincide with the weakening of the Caribbean Low Level Jet (CLLJ). The CLLJ is characterized by a predominantly easterly wind with a maximum at the central Caribbean Sea between 12°–16 °N and 71°–76°W. This low level jet increases vertical shear which reduces convection in June-July and December-March (Amador 1998; Wang 2007; Amador 2008; Muñoz et al. 2008), coinciding with the two lightning minima observed over Lake Maracaibo (Figure 3b). The weakening of CLLJ in September-November and May (as a response from the smaller gradient in sea level pressure and sea surface temperature in the Caribbean Sea) favours convection and is responsible for the rainy season over northern South America and southern Central America (Mapes et al. 2003b; Muñoz et al. 2008). This decrease in vertical shear increases air mass thunderstorm development in Lake Maracaibo contributing to the frequent lightning activity in August to October and April to May.

The persistent low-level convergence over the warm waters of Lake Maracaibo almost all year long is a perfect scenario for development of thunderstorms and lightning production which contributes to the observed high FRD. Nocturnal convection and lightning activity over Lake Maracaibo have been reported in the literature by previous authors (Mapes et al. 2003b; Martinez et al. 2003; Albrecht et al. 2011a; Falcon 2011; Bürgesser et al. 2012). Several other inland lakes with similar conditions, i.e., deep nocturnal convection driven by locally forced convergent flow over a warm lake surface, were identified in the LIS climatology. Lake Victoria, in Africa, is one of them. It is the largest tropical lake in the world, with an area of approximately 68,800 km^2. This lake is located east of the Mitumba Mountains, in between the two branches of Rift Valley, and is divided among Tanzania, Uganda and Kenya. As with Lake Maracaibo, Lake Victoria lightning activity is more pronounced during the night. Maximum convection and rainfall occurring during the night to early morning has long been recognized by studies dating from the 1960's. This nightime maximum has been attributed to convergent nocturnal land breezes (e.g., Flohn and Fraedrich 1966; Ba and Nicholson 1998; Yin and Nicholson 2000; Nicholson and Yin 2002). Ba and Nicholson (1998) found that maximum convection occurs during the morning (0500-0800 LST) with a second peak in the afternoon, while over the surrounding land maximum convection is observed in the afternoon and evening. These findings are corroborated by the daytime and nighttime FRD over Lake Victoria shown in Figure 6b. According to Flohn and Fraedrich (1966) and Nicholson and Yin (2002), due to prevailing easterly low level winds, convection generally moves from the eastern surrounding land in the late afternoon towards the northeastern portion and center of the lake during the night, and then towards the western portion of the lake during late night and early afternoon. In addition, other African Rift Valley lakes such as Tanganyika, Malawi and Albert show nocturnal convergent land breeze (Nicholson and Yin 2002) with the LIS lightning activity peaks during the late night and early morning (Figure 1b).

SUMMARY AND CONCLUSIONS

Sixteen years of TRMM LIS lightning measurements are used to construct a very high resolution (0.1°) total (cloud-to-ground and intracloud) lightning climatology. The derived lightning flash rate density maps reconfirm the previous general observations of continental deep convection over land and reduced lightning activity over the ocean with greater detail on mountainous regions such as the Andes, Himalayas, Sierra Madre and Mitumba Mountains in Africa, all of which are marked by the frequent occurrence of thunderstorms at their foothills. The diurnal cycle over most continental regions presents lightning maximum during the afternoon, with exceptions driven by locally forced circulations (such as mountain-valley and land-lake breezes) and nocturnal development of MCSs. The month of maximum flash rate density shows most lightning occurrence during summer months, except for strong monsoonal regions, as with India and the Amazon, where lightning maximum activity occurs during springtime (pre-monsoon months), and in case of India, also in the post-monsoon months.

Finally, we identify the Earth's lightning hotspots by ranking the climatological flash rate density, as well as the top ten hotspots of each continental landmass, to highlight details of their annual and diurnal cycle of lightning activity. Earth's top-ranked lightning hotspot occurs over

Lake Maracaibo in Venezuela where lightning occurs 297 days per year (with a peak in September) due to convergent land breeze over this hot lake. Lake Victoria, as well as other lakes along the east African Rift Valley, exhibit deep nocturnal convective activity driven by locally forced land breezes. The second ranked lightning hotspot on Earth is at Kahuzi-Biéga National Park, near the city of Kabare in Democratic Republic of Congo on the west side of the Mitumba Mountains. Several African lightning maxima are located along this mountain range, with strong afternoon lightning activity all year long with peaks in March and September. Asia's lightning hotspot is at northwestern ridges of the Himalayas, near Daggar, Pakistan. Its annual and diurnal cycles show maximum activity, respectively, in the summer and late afternoon to early evening. North America and Oceania top lightning hotspots are, respectively, at Patulul, Guatemala, and Derby, Australia, with afternoon and summer maximums. In the United States, the lightning hotspot is at the Everglades, near Orangetree, Florida, ranked in fourteenth position in North America and 122th globally.

Court and Griffiths (1983) found that the place in the world with more thunderstorms per day was in Uganda (242), followed by Democratic Republic of Congo (former Zaire) (228) and Rwanda (221). These last two locations are within 200 km from Kabare, CD, the second Earth's hotspot found in the current study. Unfortunately, they did not have data from Venezuela. Court and Griffiths (1983) also observed that most thunderstorms days were associated with complex terrain and coastal lines, and stated: "There is a relation, although not perfect, with topography, land-sea configuration, airmass movements and airflow on all scales.". In fact, from the first 30 lightning hotspots only 6 are not near mountainous regions. For example, the strongest hotspots from each continental landmass are near or related to mountainous regions: Lake Maracaibo in South America, Kabare in Africa, Daggar (Pakistan) in Asia, and Patulul (Guatemala) in North

America, with the exception being Oceania's top hotspot occurs in Derby (Australia) within a flat coast region. These features are so localized that they are only recognized when looking at the fine scales of the interaction between wind and complex terrain that leads to cloud development. Nesbitt and Anders (2009) and Biasutti et al. (2011) explored TRMM Precipitation Radar climatologies at very high resolutions (0.1º and 0.05º, respectively) to investigate the role of topography and coastlines affecting tropical rainfall distributions. Nesbitt and Anders (2009) found high precipitation accumulations over narrow bands from 500 to 2000 m in elevation at the eastward foothills of the Andes, as well as a distinctly drier region along high (>2000 m) slopes of the northern portion and Altiplano to the south. Here, lightning activity in very high terrain is also very low (< 2 fl km^{-2} yr^{-1}) or absent distinctly marking the Andes mountain ranges along the South America west coast, the Sierra Madre in Mexico, and the Himalayas in Asia. One noticeable exception is the northern range over Colombia and Venezuela. Whereas most of the accumulated precipitation is found west of the Andes towards the ocean (Mapes et al. 2003b; Nesbitt and Anders 2009; Biasutti et al. 2011) lightning activity is concentrated within the several valleys between the mountain ranges, marking two distinct regimes of rain yield per flash: high precipitation rates and moderate lightning activity towards the ocean (high rain yield per flash), and high precipitation rates and high FRD along the valleys (low rain yield per flash) (Takayabu 2006).

After over 17 years of operational service, the TRMM mission came to a close as the satellite used up its fuel and began a slow orbital descent that began in October 2014 and ended when the LIS instrument was powered off on April 8, 2015 when TRMM reached its decommissioning altitude of 335 km. This and all previous work related to TRMM LIS and OTD has proven the excellent Low Earth Orbit lightning measurements. To extend the continuity of these measurements, a space-qualified LIS, built as the flight spare for TRMM, will be launched on a science mission to the International Space Station (ISS) in an orbit altitude similar to TRMM LIS, 425 km. The ISS LIS is expected to be launched and placed in operation aboard the ISS in mid- 2016 (Blakeslee et al. 2014). Moreover, in October 2016 the next generation of NOAA geostationary satellites, the GOES-R series, will be launched with the first Geostationary Lightning Mapper (GLM) that will provide unprecedented continuous day and night total lightning observations from geostationary orbit and extend the climate data set begun with OTD and TRMM LIS for another 20-30 years. Therefore, the present study provides insight and context to forecasters and researchers who will use total lightning activity to better understand the earth around us.

Acknowledgments

We would like to acknowledge the support of the NASA Earth Science Division and the NOAA GOES-R Science Office in addition to the work of all LIS Science Team members. All past and current members have contributed in some degree to the success of this mission. A special thanks is offered to Dennis Boccippio who developed the source code for OTD and LIS gridded climatologies, which were modified here to obtain the very high resolution grid (0.1^{o}) results. We also thank the editor, Edward Zipser, and three anonymous reviewers for their helpful comments and suggestions. Douglas Mach (USRA), thank you for the discussions on LIS algorithm and flash length. LIS data used in this work and the gridded climatologies produced here are distributed by the NASA EOSDIS Global Hydrology Resource Center DAAC, Huntsville, AL, USA, http://thunder.nsstc.nasa.gov. The views, opinions, and findings contained in this report are those of the authors.

References

Albrecht, R. I., S. J. Goodman, W. A. Petersen, D. E. Buechler, E. C. Bruning, and R. J. Blakeslee, 2011a: The 13 years of TRMM Lightning Imaging Sensor : From individual flash characteristics to decadal tendencies. *XIV International Conference on Atmospheric Electricity*, Rio de Janeiro, Brazil, 1–4.

Albrecht, R. I., C. A. Morales, and M. A. F. Silva Dias, 2011b: Electrification of precipitating systems over the Amazon: Physical processes of thunderstorm development. *J. Geophys. Res.*, **116**, D08209, doi:10.1029/2010JD014756.

——, D. J. Cecil, and S. J. Goodman, 2014: Encyclopedia of Remote Sensing. *Encyclopedia of Remote Sensing SE - 86*, E.G. Njoku, Ed., *Encyclopedia of Earth Sciences Series*, Springer New York, New York, NY, 339–344.

Amador, J. a., 1998: A Climatic Feature of he Tropical Amerias: The Trade Winde Eatserly Jet. *Top. Meteorol. y Oceanogr.*, **5**, 91–102.

——, 2008: The Intra-Americas Sea low-level jet: Overview and future research. *Annals of the New York Academy of Sciences*, Vol. 1146 of, 153–188.

Ba, M. B., and S. E. Nicholson, 1998: Analysis of Convective Activity and Its Relationship to the Rainfall over the Rift Valley Lakes of East Africa during 1983–90 Using the Meteosat Infrared Channel. *J. Appl. Meteorol.*, **37**, 1250–1264, doi:10.1175/1520-0450(1998)037<1250:AOCAAI>2.0.CO;2.

Balas, N., and S. Nicholson, 2007: The relationship of rainfall variability in West Central Africa to sea- surface temperature fluctuations. *Int. J.*, **1349**, 1335–1349, doi:10.1002/joc.

Barros, a. P., G. Kim, E. Williams, and S. W. Nesbitt, 2004: Probing orographic controls in the Himalayas during the monsoon using satellite imagery. *Nat. Hazards Earth Syst. Sci.*, **4**, 29–51, doi:10.5194/nhess-4-29-2004.

Barros, A. P., and T. J. Lang, 2003: Monitoring the Monsoon in the Himalayas: Observations in Central Nepal, June 2001. *Mon. Weather Rev.*, **131**, 1408–1427, doi:10.1175/1520-0493(2003)131<1408:MTMITH>2.0.CO;2.

Biasutti, M., S. E. Yuter, C. D. Burleyson, and A. H. Sobel, 2011: Very high resolution rainfall patterns measured by TRMM precipitation radar: seasonal and diurnal cycles. *Clim. Dyn.*, **39**, 239–258, doi:10.1007/s00382-011-1146-6.

Blakeslee, R. J., and Coauthors, 2014: Lightning Imaging Sensor (LIS) for the International Space Station (ISS): Mission Description and Science Goals. *XV International Conference on Atmospheric Electricity*, Norman, OK, USA.

Boccippio, D. J., S. J. Goodman, and S. J. Heckman, 2000: Regional differences in tropical lightning distributions. *J. Appl. …*, **39**, 2231–2248, doi:10.1175/1520-

0450(2001)040<2231:RDITLD>2.0.CO;2.

Brooks, C. E. P., 1925: The distribution of thunderstorms over the globe. *Geophys. Mem. London*, **24**, 147–164.

Buechler, D. E., W. J. Koshak, H. J. Christian, and S. J. Goodman, 2014: Assessing the performance of the Lightning Imaging Sensor (LIS) using Deep Convective Clouds. *Atmos. Res.*, **135-136**, 397–403, doi:10.1016/j.atmosres.2012.09.008.

Bürgesser, R. E., M. G. Nicora, and E. E. Ávila, 2012: Characterization of the lightning activity of "Relámpago del Catatumbo." *J. Atmos. Solar-Terrestrial Phys.*, **77**, 241–247, doi:10.1016/j.jastp.2012.01.013.

Cecil, D. J., and C. B. Blankenship, 2012: Toward a Global Climatology of Severe Hailstorms as Estimated by Satellite Passive Microwave Imagers. *J. Clim.*, **25**, 687–703, doi:10.1175/JCLI-D-11-00130.1.

——, S. J. Goodman, D. J. Boccippio, E. J. Zipser, and S. W. Nesbitt, 2005: Three Years of TRMM Precipitation Features. Part I: Radar, Radiometric, and Lightning Characteristics. *Mon. Weather Rev.*, **133**, 543–566, doi:10.1175/MWR-2876.1.

——, D. E. Buechler, and R. J. Blakeslee, 2014: Gridded lightning climatology from TRMM-LIS and OTD: Dataset description. *Atmos. Res.*, **135-136**, 404–414, doi:10.1016/j.atmosres.2012.06.028.

Christian, H. J., R. J. Blakeslee, and S. J. Goodman, 1992: *Lightning Imaging Sensor (LIS) for the Earth Observing System*. Huntsville, AL, 36 pp.

——, and Coauthors, 2003: Global frequency and distribution of lightning as observed from space by the Optical Transient Detector. *J. Geophys. Res.*, **108**, 4005, doi:10.1029/2002JD002347.

Codazzi, A., 1841: *Resúmen de la geografía de Venezuela*. Paris, Impr. de H. Fournier y compia, 661 pp.

Court, A., and J. F. Griffiths, 1983: Thunderstorm Climatology. *Thunderstorm Morphology and Dynamics of Thunderstorms: A Social, Scientific, and Technological Documentary*, E. Kessler, Ed., University of Oklahoma Press, Norman, 11–52.

Falcon, N., 2011: Phenomenology and microphysics of lightning flash of the Catatumbo River (Venezuela). *Proceedings of the 14th International Conference on Atmospheric Electricity - ICAE*, 1–4.

Flohn, H., and K. Fraedrich, 1966: Tagesperiodische Zirkulation und Niederschlagsverteilung am Victoria-See (Ostafrika) (The daily periodic circulation and distribution of rainfall over Lake Victoria, in German). *Meteorol. Rundschau*, **19**, 157–165.

Futyan, J. M., and A. D. Del Genio, 2007: Relationships between lightning and properties of convective cloud clusters. *Geophys. Res. Lett.*, **34**, L15705, doi:10.1029/2007GL030227.

Garreaud, R., and J. M. Wallace, 1997: The Diurnal March of Convective Cloudiness over the Americas. *Mon. Weather Rev.*, **125**, 3157–3171, doi:10.1175/1520-0493(1997)125<3157:TDMOCC>2.0.CO;2.

Goodman, S., D. Buechler, and E. McCaul, 2007: Lightning. *Our Changing Planet: The View from Space*, M. King, C. Parkinson, K. Partington, and R. Williams, Eds., Cambridge University Press, 44–52.

Goodman, S. J., and H. J. Christian, 1993: Global observations of lightning. *Atlas of satellite observations related to global change*, R.J. Gurney, J.L. Foster, and C.L. Parkinson, Eds., Cambridge University Press, 191–219.

——, D. E. Buechler, K. Knupp, K. Driscoll, and E. W. McCaul, 2000: The 1997-98 El Nino event and related wintertime lightning variations in the southeastern United States. *Geophys. Res. Lett.*, **27**, 541–544, doi:10.1029/1999GL010808.

Heckman, S. J., E. Williams, and B. Boldi, 1998: Total global lightning inferred from Schumann resonance measurements. *J. Geophys. Res.*, **103**, 31775, doi:10.1029/98JD02648.

Houze, R. A., D. C. Wilton, and B. F. Smull, 2007: Monsoon convection in the Himalayan region as seen by the TRMM Precipitation Radar. *Q. J. R. Meteorol. Soc.*, **133**, 1389–1411, doi:10.1002/qj.106.

Jackson, B., S. E. Nicholson, and D. Klotter, 2009: Mesoscale Convective Systems over Western Equatorial Africa and Their Relationship to Large-Scale Circulation. *Mon. Weather Rev.*, **137**, 1272–1294, doi:10.1175/2008MWR2525.1.

Jayaratne, E. R., and Y. Kuleshov, 2006: Geographical and seasonal characteristics of the relationship between lightning ground flash density and rainfall within the continent of Australia. *Atmos. Res.*, **79**, 1–14, doi:10.1016/j.atmosres.2005.03.004.

Kandalgaonkar, S. S., 2003: Diurnal variation of lightning activity over the Indian region. *Geophys. Res. Lett.*, **30**, 2022, doi:10.1029/2003GL018005.

——, 2005: Spatio-temporal variability of lightning activity over the Indian region. *J. Geophys. Res.*, **110**, D11108, doi:10.1029/2004JD005631.

Kodama, Y.-M., A. Ohta, M. Katsumata, S. Mori, S. Satoh, and H. Ueda, 2005: Seasonal transition of predominant precipitation type and lightning activity over tropical monsoon areas derived from TRMM observations. *Geophys. Res. Lett.*, **32**, n/a – n/a, doi:10.1029/2005GL022986.

Kotaki, M., 1984: Global distribution of atmospheric radio noise derived from thunderstorm activity. *J. Atmos. Terr. Phys.*, **46**, 867–877, doi:10.1016/0021-9169(84)90026-6.

Kuleshov, Y., D. Mackerras, and M. Darveniza, 2006: Spatial distribution and frequency of lightning activity and lightning flash density maps for Australia. *J. Geophys. Res.*, **111**, D19105, doi:10.1029/2005JD006982.

Laing, A. G., and J. M. Fritsch, 1993: Mesoscale Convective Complexes in Africa. *Mon. Weather Rev.*, **121**, 2254–2263, doi:10.1175/1520-0493(1993)121<2254:MCCIA>2.0.CO;2.

——, and J. M. Fritsch, 1997: The global population of mesoscale convective complexes. *Q. J. R. Meteorol. Soc.*, **123**, 389–405, doi:10.1002/qj.49712353807.

Lal, D. M., and S. D. Pawar, 2009: Relationship between rainfall and lightning over central Indian region in monsoon and premonsoon seasons. *Atmos. Res.*, **92**, 402–410, doi:10.1016/j.atmosres.2008.12.009.

Liu, C., D. Cecil, and E. J. Zipser, 2011: Relationships between lightning flash rates and passive microwave brightness temperatures at 85 and 37 GHz over the tropics and subtropics. *J. Geophys. Res. Atmos.*, **116**, n/a – n/a, doi:10.1029/2011JD016463.

Lott, N., R. Vose, S. a Del Greco, T. F. Ross, S. Worley, and J. Comeaux, 2008: The Integrated Surface Database: Partnerships and Progress. *Proceedings of the 24th Conference in IIPS*.

Mackerras, D., M. Darveniza, R. E. Orville, E. R. Williams, and S. J. Goodman, 1998: Global lightning: Total, cloud and ground flash estimates. *J. Geophys. Res.*, **103**, 19791, doi:10.1029/98JD01461.

Mapes, B. E., T. T. Warner, and M. Xu, 2003a: Diurnal Patterns of Rainfall in Northwestern South America. Part III: Diurnal Gravity Waves and Nocturnal Convection Offshore. *Mon. Weather Rev.*, **131**, 830–844, doi:10.1175/1520-0493(2003)131<0830:DPORIN>2.0.CO;2.

——, ——, ——, and A. J. Negri, 2003b: Diurnal Patterns of Rainfall in Northwestern South America. Part I: Observations and Context. *Mon. Weather Rev.*, **131**, 799–812, doi:10.1175/1520-0493(2003)131<0799:DPORIN>2.0.CO;2.

Martinez, M., J. Ramirez, and R. Montano, 2003: Actividad de rayos en Venezuela, utilizando la data del sensor óptico (LIS) del proyecto TRMM de la NASA. *Rev. Téc. Ing. Univ. Zulia [online]*, **26**, 127–139.

Muñoz, E., A. J. Busalacchi, S. Nigam, and A. Ruiz-Barradas, 2008: Winter and summer structure of the Caribbean low-level jet. *J. Clim.*, **21**, 1260–1276, doi:10.1175/2007JCLI1855.1.

Negri, A. J., E. N. Anagnostou, and R. F. Adler, 2000: A 10-yr Climatology of Amazonian Rainfall Derived from Passive Microwave Satellite Observations. *J. Appl. Meteorol.*, **39**, 42–56, doi:10.1175/1520-0450(2000)039<0042:AYCOAR>2.0.CO;2.

Nesbitt, S. W., and E. J. Zipser, 2003: The Diurnal Cycle of Rainfall and Convective Intensity according to Three Years of TRMM Measurements. *J. Clim.*, **16**, 1456–1475, doi:10.1175/1520-0442(2003)016<1456:TDCORA>2.0.CO;2.

Nesbitt, S. W., and A. M. Anders, 2009: Very high resolution precipitation climatologies from the Tropical Rainfall Measuring Mission precipitation radar. *Geophys. Res. Lett.*, **36**, n/a – n/a, doi:10.1029/2009GL038026.

Nicholson, S., and X. Yin, 2002: Mesoscale Patterns of Rainfall, Cloudiness and Evaporation over the Great Lakes of East Africa. *The East African Great Lakes: Limnology, Palaeolimnology and Biodiversity SE - 3*, E. Odada and D. Olago, Eds., Vol. 12 of *Advances in Global Change Research*, Springer Netherlands, 93–119.

Nicholson, S. E., 1996: A review of climate dynamics and climate variability in Eastern Africa. *Limnology, Climatology and Paleoclimatology of the East African Lakes*.

Nicholson, S. E., 2009: A revised picture of the structure of the "monsoon" and land ITCZ over West Africa. *Clim. Dyn.*, **32**, 1155–1171, doi:10.1007/s00382-008-0514-3.

——, and J. P. Grist, 2003: The seasonal evolution of the atmospheric circulation over West Africa and equatorial Africa. *J. Clim.*, **16**, 1013–1030, doi:10.1175/1520-0442(2003)016<1013:TSEOTA>2.0.CO;2.

Orville, R. E., and R. W. Henderson, 1986: Global Distribution of Midnight Lightning: September 1977 to August 1978. *Mon. Weather Rev.*, **114**, 2640–2653, doi:10.1175/1520-0493(1986)114<2640:GDOMLS>2.0.CO;2.

Petersen, W. a., H. J. Christian, and S. a. Rutledge, 2005: TRMM observations of the global relationship between ice water content and lightning. *Geophys. Res. Lett.*, **32**, n/a – n/a, doi:10.1029/2005GL023236.

Petersen, W. A., R. Fu, M. Chen, and R. Blakeslee, 2006: Intraseasonal Forcing of Convection and Lightning Activity in the Southern Amazon as a Function of Cross-Equatorial Flow. *J. Clim.*, **19**, 3180–3196, doi:10.1175/JCLI3788.1.

Poveda, G., and Coauthors, 2005: The Diurnal Cycle of Precipitation in the Tropical Andes of Colombia. *Mon. Weather Rev.*, **133**, 228–240, doi:10.1175/MWR-2853.1.

Pulwarty, R. S., R. G. Barry, C. M. Hurst, K. Sellinger, and L. F. Mogollon, 1998: Precipitation in the Venezuelan Andes in the context of regional climate. *Meteorol. Atmos. Phys.*, **67**, 217–237, doi:10.1007/BF01277512.

Rasmussen, K. L., and R. a. Houze, 2011: Orogenic Convection in Subtropical South America as Seen by the TRMM Satellite. *Mon. Weather Rev.*, **139**, 2399–2420, doi:10.1175/MWR-D-10-05006.1.

Rasmussen, K. L., M. D. Zuluaga, and R. A. Houze, 2014: Severe convection and lightning in subtropical South America. *Geophys. Res. Lett.*, **41**, 7359–7366, doi:10.1002/2014GL061767.

Takayabu, Y. N., 2006: Rain-yield per flash calculated from TRMM PR and LIS data and its relationship to the contribution of tall convective rain. *Geophys. Res. Lett.*, **33**, 1–4, doi:10.1029/2006GL027531.

Virts, K. S., J. M. Wallace, M. L. Hutchins, and R. H. Holzworth, 2013: Highlights of a New Ground-Based, Hourly Global Lightning Climatology. *Bull. Am. Meteorol. Soc.*, **94**, 1381–1391, doi:10.1175/BAMS-D-12-00082.1.

Wang, C., 2007: Variability of the Caribbean Low-Level Jet and its relations to climate. *Clim. Dyn.*, **29**, 411–422, doi:10.1007/s00382-007-0243-z.

Williams, E., 2002: Contrasting convective regimes over the Amazon: Implications for cloud electrification. *J. Geophys. Res.*, **107**, 1–19, doi:10.1029/2001JD000380.

Williams, E., 2004: Islands as miniature continents: Another look at the land-ocean lightning contrast. *J. Geophys. Res.*, **109**, D16206, doi:10.1029/2003JD003833.

——, and S. Stanfill, 2002: The physical origin of the land–ocean contrast in lightning activity. *Comptes Rendus Phys.*, **3**, 1277–1292, doi:10.1016/S1631-0705(02)01407-X.

Williams, E., K. Rothkin, D. Stevenson, and D. Boccippio, 2000: Global Lightning Variations Caused by Changes in Thunderstorm Flash Rate and by Changes in the Number of Thunderstorms. *J. Appl. Meteorol.*, **39**, 2223–2230, doi:10.1175/1520-0450(2001)040<2223:GLVCBC>2.0.CO;2.

Williams, E. R., and S. J. Heckman, 1993: The local diurnal variation of cloud electrification and the global diurnal variation of negative charge on the Earth. *J. Geophys. Res.*, **98**, 5221, doi:10.1029/92JD02642.

WMO (World Meteorological Society), 1953: World Distribution of thunderstorm days. Publ. 21, TP. 6 and supplement (1956).

Yin, X., and S. E. Nicholson, 2000: On the diurnal cycle of cloudiness over Lake Victoria and its influence on evaporation from the lake. **45**.

Zipser, E. J., C. Liu, D. J. Cecil, S. W. Nesbitt, and D. P. Yorty, 2006: Where Are the Most Intense Thunderstorms on Earth? *Bull. Am. Meteorol. Soc.*, **87**, 1057–1071, doi:10.1175/BAMS-87-8-1057.

Tables (w/ captions above, one per page)

Table 1 – Top 10 flash rate density (FRD, fl km^{-2} yr^{-1}) for each continent landmass, indicating its position in the global ranking, latitude (Lat) and longitude (Lon) position on TRMM LIS 0.1^{o} climatology grid, as well as the name of the nearest populated place name (PPL), position (PPL Lat, PPL Lon) and distance from grid point (Dist.) according to Geonames.org. A minimum distance of 100km from a previous ranked grid point was applied.

Global Rank	FRD	Lat (°)	Lon (°)	PPL	Country	PPL Lat (°)	PPL Lon (°)	Dist. (km)
South America								
1	232.52	9.75	-71.65	Lake Maracaibo (Lagunillas)	Venezuela	10.13	-71.26	60.1
4	172.29	7.55	-75.35	Cáceres	Colombia	7.58	-75.35	3.4
7	138.61	8.85	-73.05	El Tarra	Colombia	8.58	-73.09	30.9
11	124.26	5.75	-74.95	Norcasia	Colombia	5.58	-74.89	20.4
18	114.19	8.45	-74.55	Majagual	Colombia	8.54	-74.62	12.6
25	105.73	8.15	-76.85	Turbo	Colombia	8.09	-76.73	14.8
46	95.38	11.15	-72.95	Barrancas	Colombia	10.96	-72.79	27.8
74	87.96	-17.25	-65.05	Chimoré	Bolivia	-16.95	-65.14	34.9
78	87.61	10.35	-70.95	El Corozo	Venezuela	10.12	-71.04	27.5
136	77.02	10.45	-75.35	Santa Rosa	Colombia	10.44	-75.37	2.2
Africa								
2	205.31	-1.85	27.75	Kabare	Dem. Rep. Congo	-2.50	28.79	136.2
3	176.71	-3.05	27.65	Kampene	Dem. Rep. Congo	-3.60	26.67	124.9
5	143.21	-0.95	27.95	Sake	Dem. Rep. Congo	-1.57	29.04	140.0
8	129.58	5.25	9.35	Nguti	Cameroon	5.33	9.42	11.7
9	129.50	0.25	28.45	Butembo	Dem. Rep. Congo	0.14	29.29	94.3
10	127.52	-1.55	20.95	Boende	Dem. Rep. Congo	-0.28	20.88	141.2
14	117.98	0.55	20.35	Boende	Dem. Rep. Congo	-0.28	20.88	109.7
15	117.19	-2.45	26.95	Kindu	Dem. Rep. Congo	-2.94	25.92	126.7
16	116.78	6.95	10.45	Baissa	Nigeria	7.23	10.63	36.6
19	112.17	0.35	26.65	Kisangani	Dem. Rep. Congo	0.52	25.19	163.3
Asia								
6	143.11	34.45	72.35	Daggar	Pakistan	34.51	72.48	14.0
12	121.41	33.35	74.55	Rājauri	India	33.38	74.31	22.6
13	118.81	33.75	70.75	Doāba	Pakistan	33.42	70.74	36.2
22	108.03	14.55	43.45	Al Ḩadīyah	Yemen	14.53	43.57	13.2
28	104.59	33.85	73.25	Murree	Pakistan	33.91	73.39	14.5
31	101.79	25.25	91.95	Cherrapunji	India	25.30	91.70	26.1
42	97.02	4.75	103.05	Paka	Malaysia	4.64	103.44	44.7
45	95.92	1.95	103.85	Kota Tinggi	Malaysia	1.74	103.90	24.2
50	94.64	3.75	98.05	Tenggulun	Indonesia	3.99	98.01	27.3
52	93.96	3.15	101.65	Kuala Lumpur	Malaysia	3.14	101.69	4.2
North America								
17	116.76	14.35	-91.15	Patulul	Guatemala	14.42	-91.17	7.6

29	103.23	14.85	-92.05	Catarina	Guatemala	14.85	-92.08	2.8
33	100.63	22.35	-83.95	San Luis	Cuba	22.29	-83.77	20.1
34	100.24	18.55	-74.35	Chambellan	Haiti	18.57	-74.32	4.0
37	99.39	13.15	-87.25	San Jerónimo	Honduras	13.18	-87.14	12.7
39	98.22	22.35	-80.65	Rodas	Cuba	22.34	-80.56	9.8
40	98.06	21.75	-78.85	Venezuela	Cuba	21.74	-78.80	5.8
47	95.32	22.85	-82.15	Mañalich	Cuba	22.81	-82.15	4.3
82	86.96	22.25	-105.25	Rosamorada	Mexico	22.12	-105.21	14.9
90	85.78	18.15	-77.65	Balaclava	Jamaica	18.17	-77.64	2.6
Oceania								
61	92.15	-15.35	125.35	Derby	Australia	-17.30	123.63	284.4
83	86.75	-14.45	126.55	Kununurra	Australia	-15.78	128.74	278.0
228	65.11	-16.65	124.75	Derby	Australia	-17.30	123.63	139.6
308	59.69	-15.65	128.45	Kununurra	Australia	-15.78	128.74	34.6
316	59.19	-4.75	142.95	Ambunti	Papua New Guinea	-4.22	142.82	61.0
327	58.57	-15.25	129.45	Kununurra	Australia	-15.78	128.74	95.8
355	57.13	-13.15	131.05	McMinns Lagoon	Australia	-12.55	131.11	66.6
381	55.57	-13.95	129.95	Darwin	Australia	-12.46	130.84	191.6
471	51.35	-19.15	137.85	Mount Isa	Australia	-20.73	139.50	245.6
477	51.22	-17.45	126.05	Halls Creek	Australia	-18.22	127.67	191.6

Figures

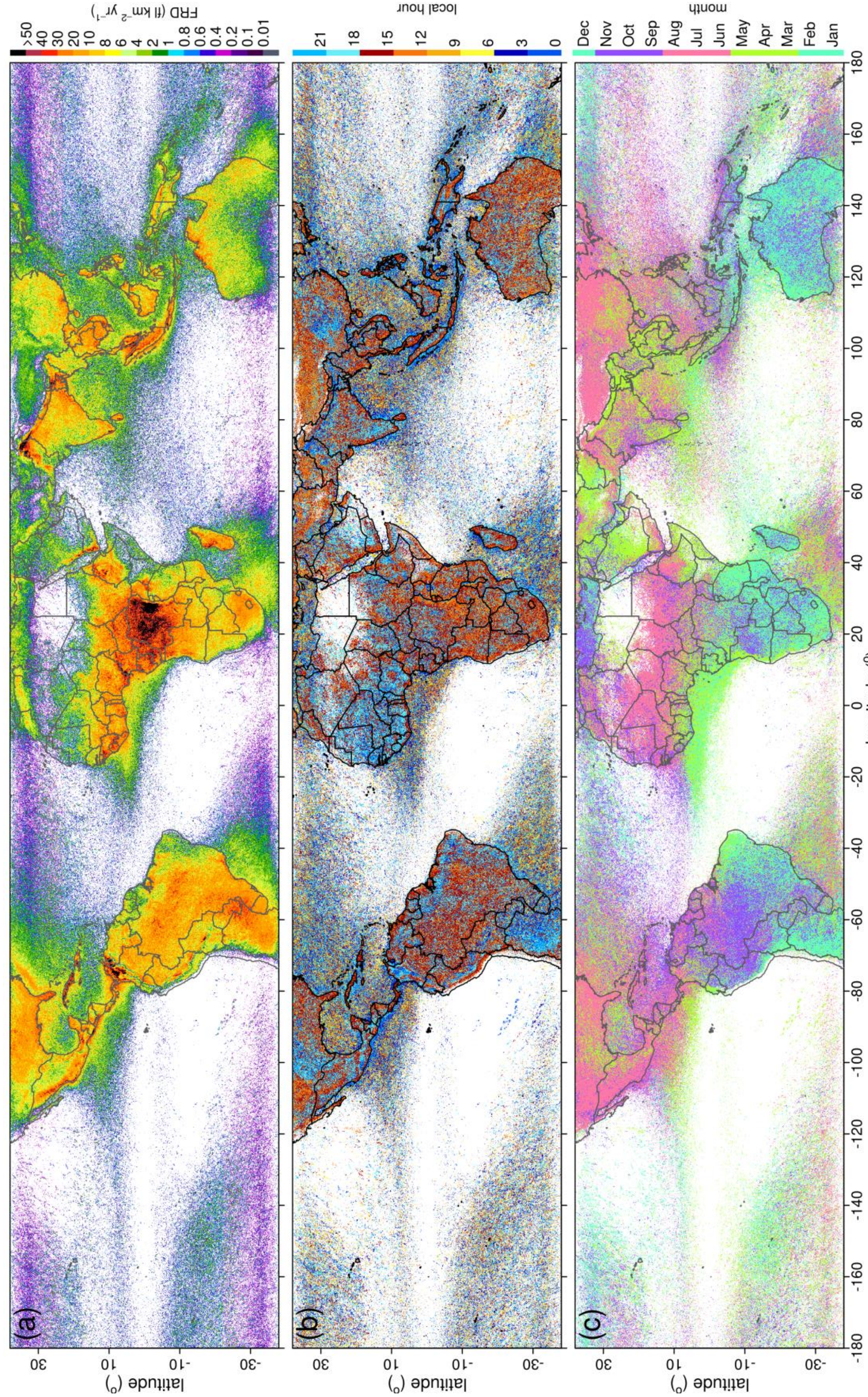

Figure 1 – Very high horizontal (0.1°) resolution total lightning climatology from 16 years (1998-2013) of TRMM LIS total lightning observations: (a) flash rate density (FRD – fl km^{-2} yr^{-1}), (b) local hour of maximum FRD, and (c) month of maximum FRD. Data shown for the latitude band of ±38°.

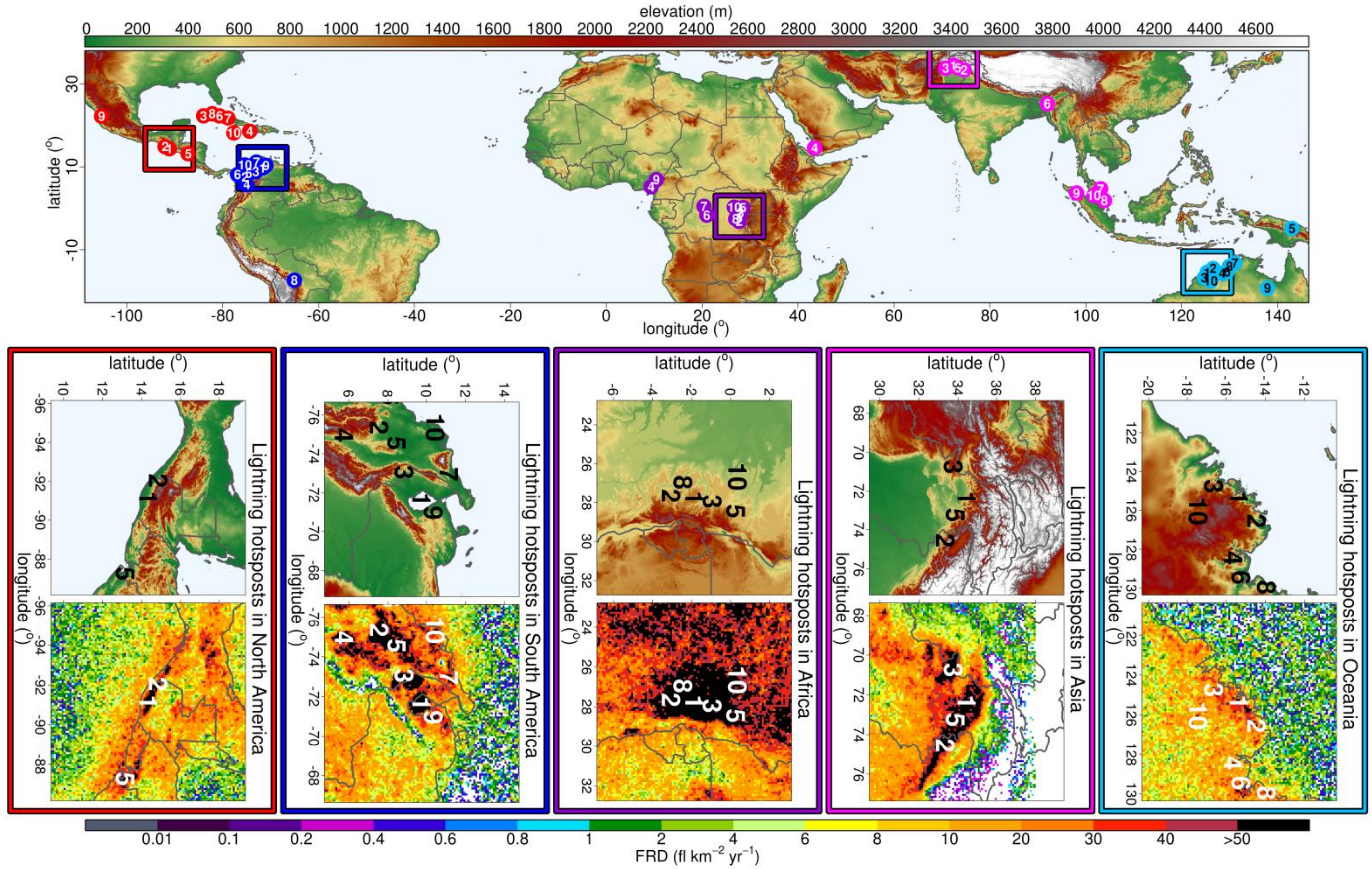

Figure 2 – (Top) Location (symbols) of the top ten FRD hotspots per major continental landmasses (Africa, Asia, North America, Oceania and South America), and (bottom) 2.5° zoom boxes on FRD climatology of each landmass first hotspot (Table 1), using the same color coding as Figure 1(a). Symbols indicate the continent landmass ranking order (1st to 10th) from Table 1, and colors indicate the continent (purple – Africa; magenta – Asia; blue- North America; light blue – Oceania; red – South America). Shaded gray scale at the top figure is terrain elevation (m), as well as the white lines (from 500 to 3000 m in 500 m intervals) on the zoom boxes of the bottom figures. Gray lines in the bottom figures are country physical boundaries.

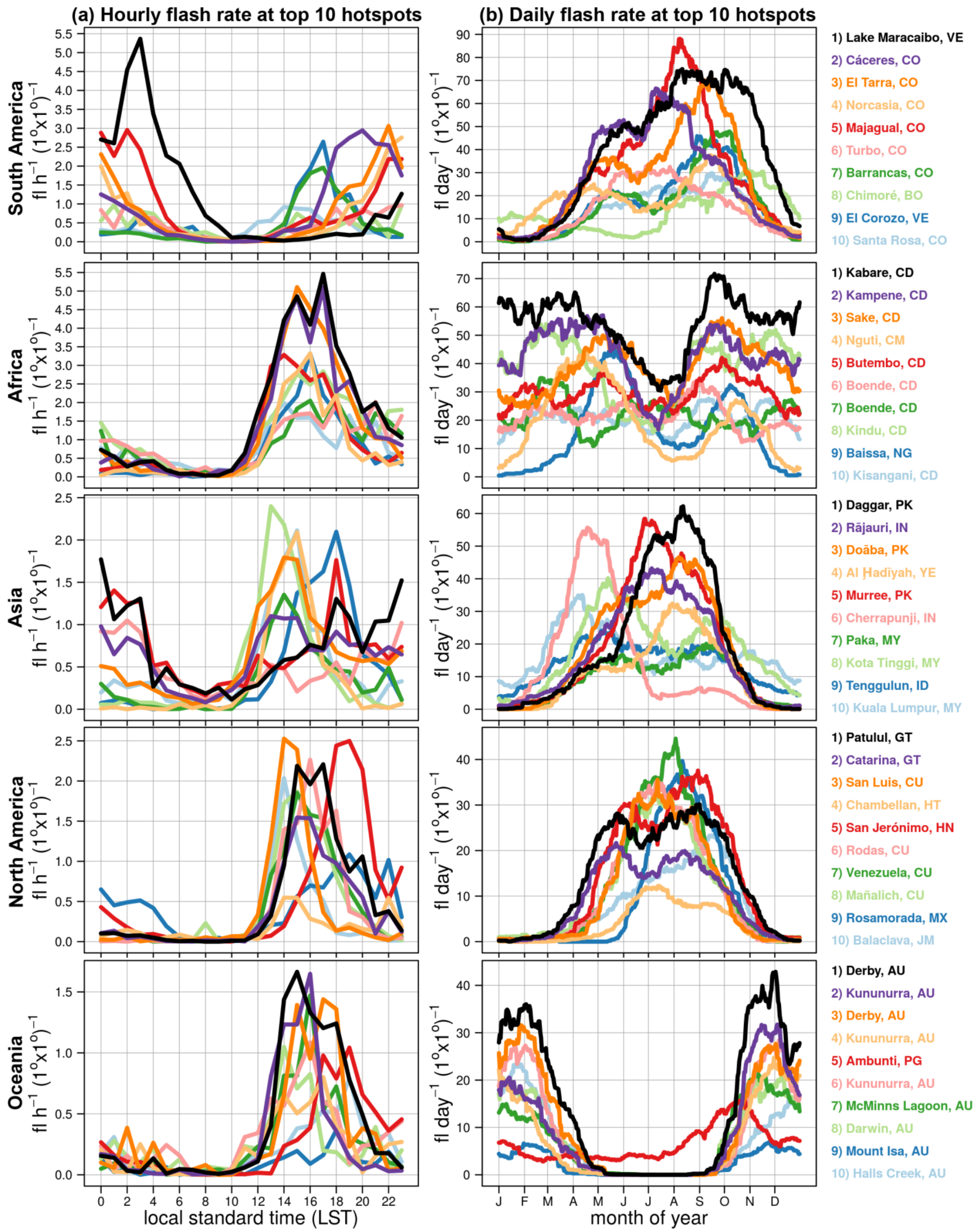

Figure 3 – (a) Hourly and (b) daily flash rate density distribution of the top ten lightning hotspots of each major continental landmass from Table 1. These values are calculated over a 1º box centered at the hotspot.

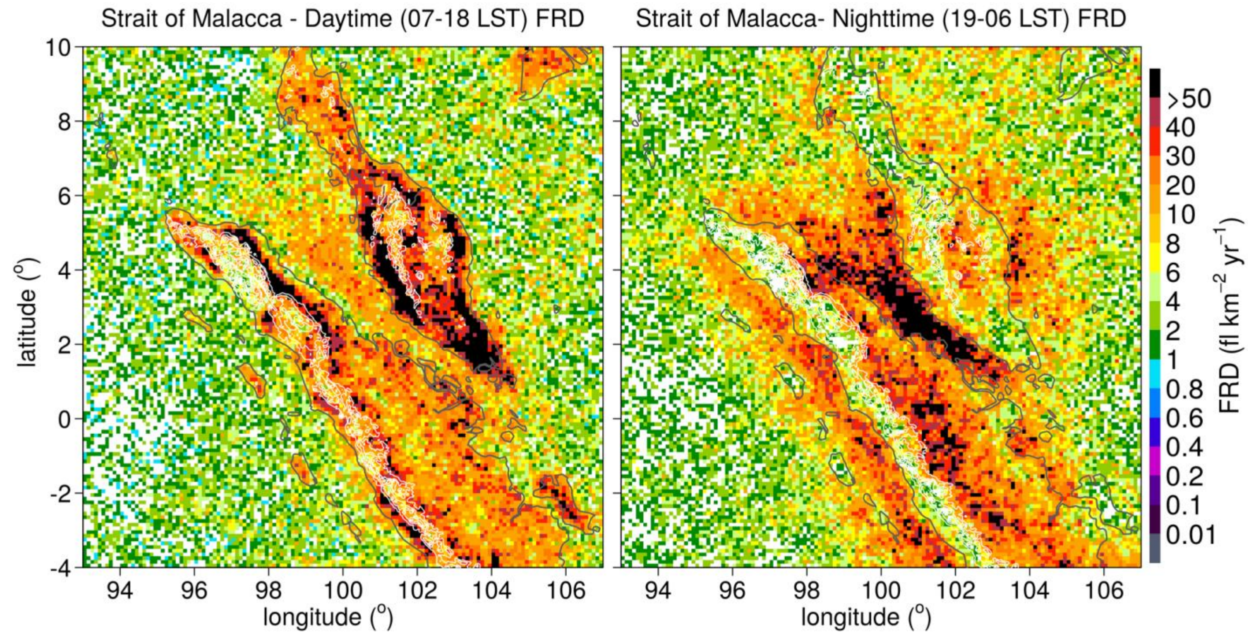

Figure 4 – Daytime (07-18 LST) and nighttime (19-06) flash rate density (fl km^2 yr^{-1}) at Strait of Malacca, Indonesia. White lines are elevation from 500 to 3000 m in 500 m intervals, and gray lines are country physical boundaries.

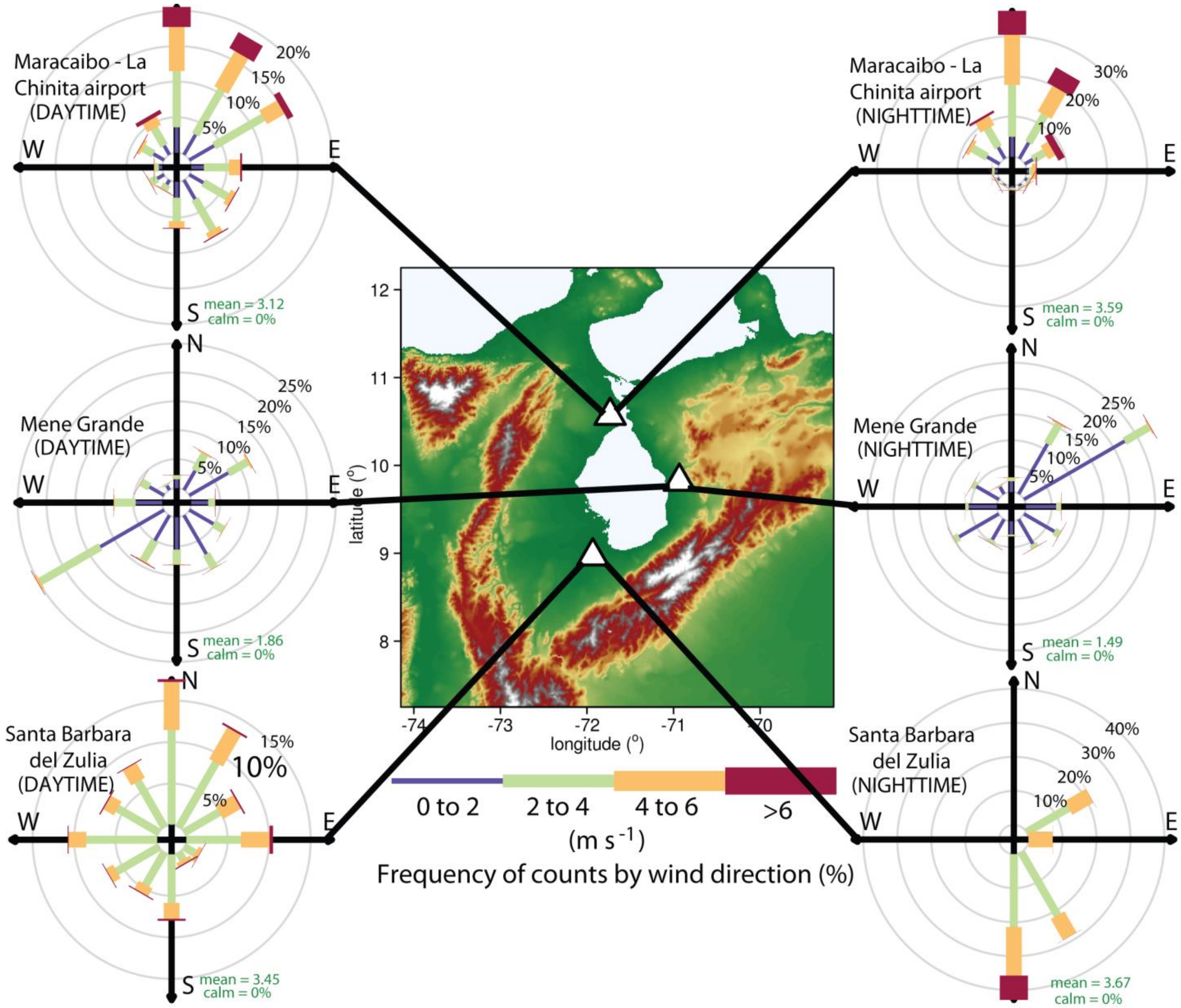

Figure 5 - Northwestern Venezuela elevation map (center), as well as daytime (left) and nighttime (right) wind roses from three locations around Lake Maracaibo: Zulia, Mene Grande and Maracaibo. Elevation color scale is the same as in Figure 2.

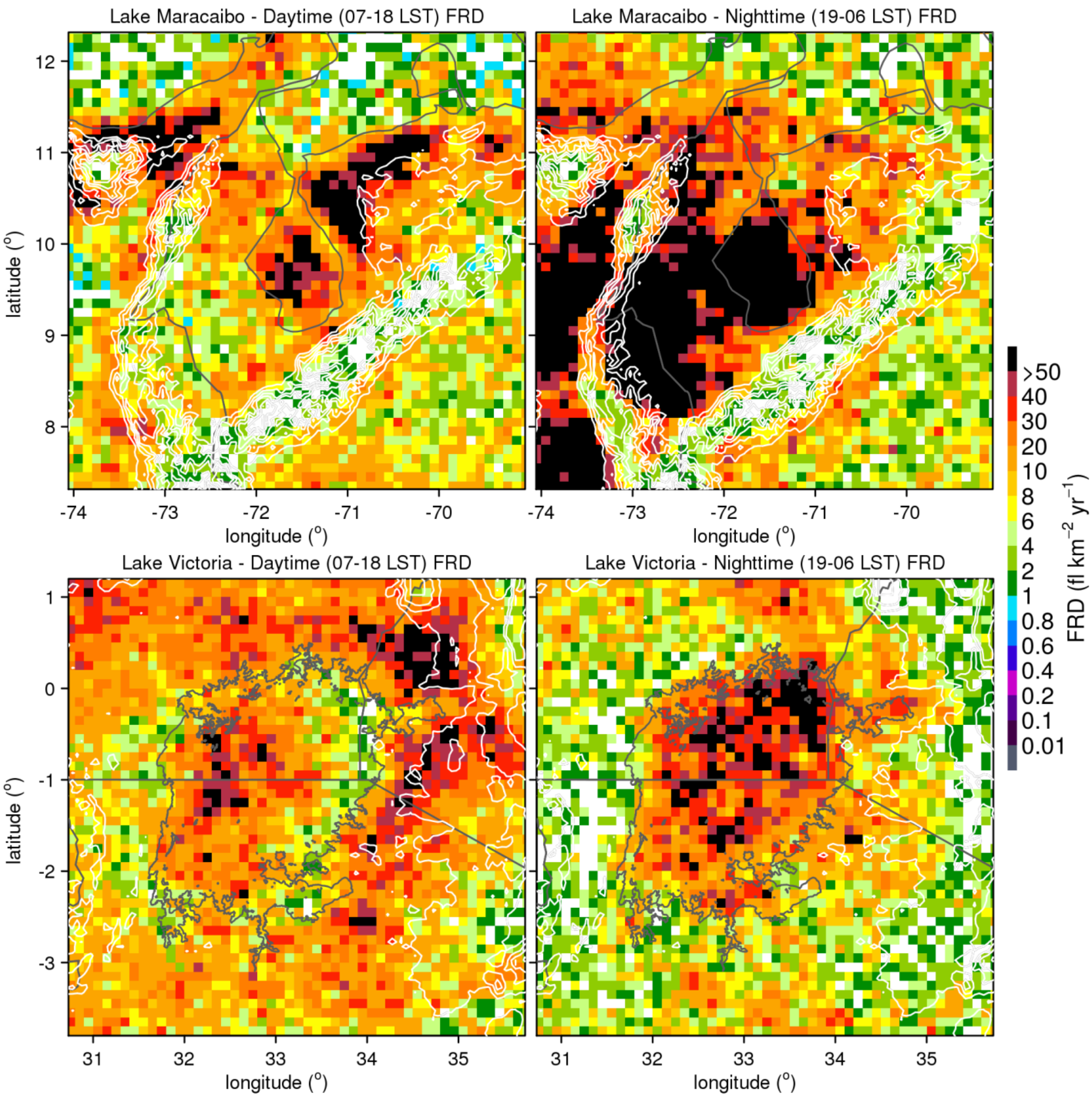

Figure 6 – Same as Figure 4, except for (top) Lake Maracaibo, Venezuela, and (bottom) Lake Victoria, Africa.